American Journal of
Biomedical Science & Research

www.biomedgrid.com
ISSN: 2642-1747

Research Article

Theoretical Investigation on N-Heterocyclic Carbene-Catalyzed Tandem Imine Umpolung-Cyclization Via Breslow Intermediate

Nan Lu*, Chengxia Miao and Xiaozheng Lan

College of Chemistry and Material Science, Shandong Agricultural University, Taian, China

***Corresponding author:** Nan Lu, College of Chemistry and Material Science, Shandong Agricultural University, Taian, China.

To Cite This Article: *Nan Lu*, Chengxia Miao and Xiaozheng Lan, Theoretical Investigation on N-Heterocyclic Carbene-Catalyzed Tandem Imine Umpolung-Cyclization Via Breslow Intermediate. Am J Biomed Sci & Res. 2024 22(1) AJBSR.MS.ID.002911,* DOI: 10.34297/AJBSR.2024.21.002911

Received: : March 25, 2024; **Published:** April 04, 2024

Abstract

The mechanism is investigated for tandem imine umpolung-cyclization of aldimine leading to isoindolinone and other two imine derivatives catalyzed by N-Heterocyclic Carbene (NHC). The aldimine is attacked by NHC generating tetrahedral intermediate, from which the intramolecular aza-Michael addition followed by H transfer gives key aza-Breslow intermediate. After oxidation by oxygen molecule, the precursor of desired N-aryl 3-isoindolinone is obtained via oxygen atom exchange from its oxidation product to itself. The alternative H transfer ahead of concerted aza-Michael addition is excluded owing to high activation energy. The preferential path is both favoured by thermodynamics and kinetics. The initial imine umpolung is consistent for other two derivatives. The following aza-Michael addition is rate-limiting. The positive solvation effect is suggested by decreased absolute and activation energies in DMSO solution compared with in gas. These results are supported by Multiwfn analysis on FMO composition of specific TSs, and MBO value of vital bonding, breaking.

Keywords: Imine umpolung, Breslow intermediate, N-Heterocyclic Carbine, aza-Michael addition, Oxygen exchange

Introduction

As privileged structural motifs, isoindolinones have been found in various natural products such as indolocarbazoles, cytochalasan alkaloids and meroterpenoids from anthraquinone-type alkaloids in intact or modified form [1]. They also emerged as active pharmaceutical ingredients to inhibit MDM2-P53 interaction and treated follicular lymphoma [2]. Particularly, N-substituted isoindolinones possess interesting biological properties. The pazinaclone is a new non-benzodiazepine compound with high affinity for benzodiazepine receptors used to alleviate anxiety [3]. With good water solubility and wide safety margin, N-aryl isoindolinone acetamide showed potent sedative-hypnotic activity [4]. Isoindolin-1-one derivative JM1232 had antinociceptive property of intrathecal and intraperitoneal administration to treat anxiolytic disorders [5]. Therefore, the development of efficient strategies has attracted considerable attention to construct such molecular skeleton. Recently, a series of isoindolinones were designed such as selective dioxane-mediated aerobic oxidation of isoindolines, intramolecular formal [4+2] cycloaddition, divergent reaction of isocyanides with o-bromobenzaldehydes, structure-guided synthetic route of PI3Kγ inhibitor and chiral brønsted acid catalyzed enantioselective [3+2] cycloaddition [6-10].

N-Heterocyclic Carbene (NHC) is versatile Lewis-base organocatalyst to facilitate cross-nucleophilic addition in C-C and C-heteroatom construction through umpolung with various electrophiles [11]. Rovis reported the isolation of aza-Breslow intermediate derived from chiral triazolylidene carbine [12]. Michon achieved chiral phase transfer-catalyzed intramolecular aza-Michael reaction with ortho-alkenyl substituted benzamide for asymmetric synthesis of isoindolinone [13]. Singh discovered a general catalytic route to enantioenriched diazo-substituted isoindolinone catalyzed by chiral phosphoric acid from the reaction of ortho-formyl benzoate, amine, and diazoacetate [14]. Recently, most efforts were devot-

ed to one-pot synthesis of isoindolinone catalyzed by transition metal including Kumar's Ru (II)-catalyzed oxidative olefination of benzamide via switchable aza-michael and aza-wacker reaction [15,16]. Biju group developed NHC-catalyzed umpolung of imine to access indole for the first time [17]. Then Lupton explored exploited the enantioselective catalysis of imine umpolung [18]. Das emphasized imines as key acceptors and donors in synthesis of amides and nitrogen heterocycles [19]. Chi researched carbene-catalyzed activation of remote N of (benz)imidazole-derived aldimines [20]. Fu studied the oxidation of functionalized aldimines as 1,4-dipoles catalyzed by asymmetric carbine [21].

In this field of NHC-catalyzed imines umpolung, what interests us the most is various organic transformation reported by Suresh group [22-24]. Based on the design principle of starting material with both imine and conjugate acceptor functional groups, they envisioned to synthesize isoindolinone acetic acid derivatives applying NHC catalysis. They successively achieved NHC-catalyzed oxidation of β-carboline cyclic imines, unactivated aldimines to amides, intramolecular stetter reaction and acid-mediated condensation. A recent breakthrough was NHC-catalyzed tandem imine umpolung-intra-molecular aza-Michael addition-oxidation to construct N-substituted isoindolinone acetate [25]. Although desired N-aryl 3-isoindolinone was obtained, there is no report about detailed mechanistic study explaining the conversion of imine to amide. What's the function of NHC in intramolecular aza-Michael addition generating aza-Breslow intermediate? How the radical recombination is proceeding with single electron transferred by molecular oxygen in air? Why is another molecule of aza-Breslow intermediate necessary to regulate the entire reaction process? To solve these mechanic problems in experiment, an in-depth theoretical study was necessary for this NHC-catalyzed tandem reaction. The Density Functional Theory (DFT) method was employed focusing on the promotion of NHC during the connection among three tandem isolated reactions.

Computational Methodology

Optimized structures were obtained at M06-2X/6-31G(d) level of theory with GAUSSIAN09 [26]. In tests of popular DFT methods [27], M06-2X functional attained smaller standard deviation of difference between calculated value and experimental value in geometries than B3LYP including Becke's three-parameter hybrid functional combined with Lee-Yang-Parr correction for correlation [28,29]. The best compromise between accuracy and time consumption was provided with 6-31G(d) basis set on energy calculations. Also, M06-2X functional was found to give relatively accurate results for catalysed enantioselective (4+3), concerted [4+2], stepwise (2+2) cycloaddition and catalysed Diels-Alder reactions [30,31]. Together with the best performance on noncovalent interaction, M06-2X functional is believed to be suitable for this system [32-34]. The nature of each structure was verified by performing harmonic vibrational frequency calculations. Intrinsic Reaction Coordinate (IRC) calculations were examined to confirm the right connections among key transition-states and corresponding reactants and products. Harmonic frequency calculations were carried out at the M06-2X/6-31G(d) level to gain Zero-Point Vibrational Energy (ZPVE) and thermodynamic corrections at 298.15 K and 1 atm for each structure in Dimethyl Sulfoxide (DMSO).

The solvation-corrected free energies were obtained at the M06-2X/6-311++G(d,p) level by using Integral Equation Formalism Polarizable Continuum Model (IEFPCM) in Truhlar's "density" solvation model [35-39] on the M06-2X/6-31G(d)-optimized geometries. As an efficient method obtaining bond and lone pair of a molecule from modern ab initio wave functions, NBO procedure was performed with Natural bond orbital (NBO3.1) to characterize electronic properties and bonding orbital interactions [40-42]. The wave function analysis was provided using Multiwfn_3.7_dev package [43] including research on Frontier Molecular Orbital (FMO) and Mayer Bond Order (MBO).

Results and Discussion

Based on previous research [21-25], the mechanism was explored for NHC-catalyzed tandem imine umpolung-cyclization of aldimine 1 leading to isoindolinone 2 compared with substrates 3 and 4 (Scheme 1).

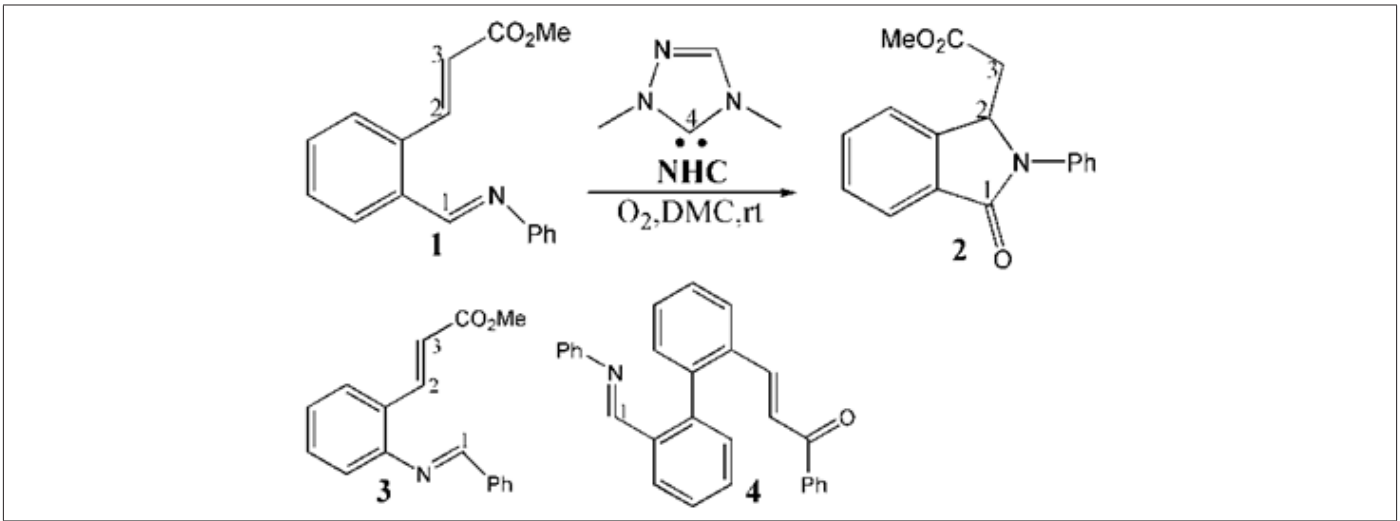

Scheme 1: N-heterocyclic carbene-catalyzed tandem imine umpolung-cyclization of aldimine 1 leading to isoindolinone 2 compared with substrates 3 and 4.

Depicted by the red arrow of Scheme 2 and illustrated by the black dash line of Figure 1a (path A), the aldimine I was attacked by nucleophilic NHC to generate a tetrahedral intermediate II. Then, intramolecular aza-Michael addition takes place followed by H transfer forming aza-Breslow intermediate III. Subsequently, III undergoes oxidation with one molecular of oxygen to produce IV, which reacts with another molecule of III affording the complex binding two molecules of intermediate V. At last, NHC departs from V producing desired product N-aryl 3-isoindolinone 2. An alternative H transfer ahead of concerted aza-Michael addition was given by red dash line of Figure 1a (path B). The generation of Breslow intermediate was also discussed for another two imine derivative 3, 4 as substrates shown by blue, green arrow of Scheme 2 and black, red dash line of Figure 1b. For both, the initial step of imine umpolung is consistent via nucleophilic addition of NHC to 3 or 4 obtaining 3-II or 4-II. Only one step of H transfer is required for 4-II leading to aza-Breslow 4-III. In contrast, the H transfer of 3-II occurs concertedly with intramolecular cyclization yielding 3-III, which is not a typical Breslow intermediate. The optimized structures of TSs in Scheme 2 were listed by Figure 2. The activation energy was shown in Table 1 for all steps. Supplementary Table S1, Table S2 provided the relative energies of all stationary points. According to experiment, the Gibbs free energies in DMSO solution phase are discussed here.

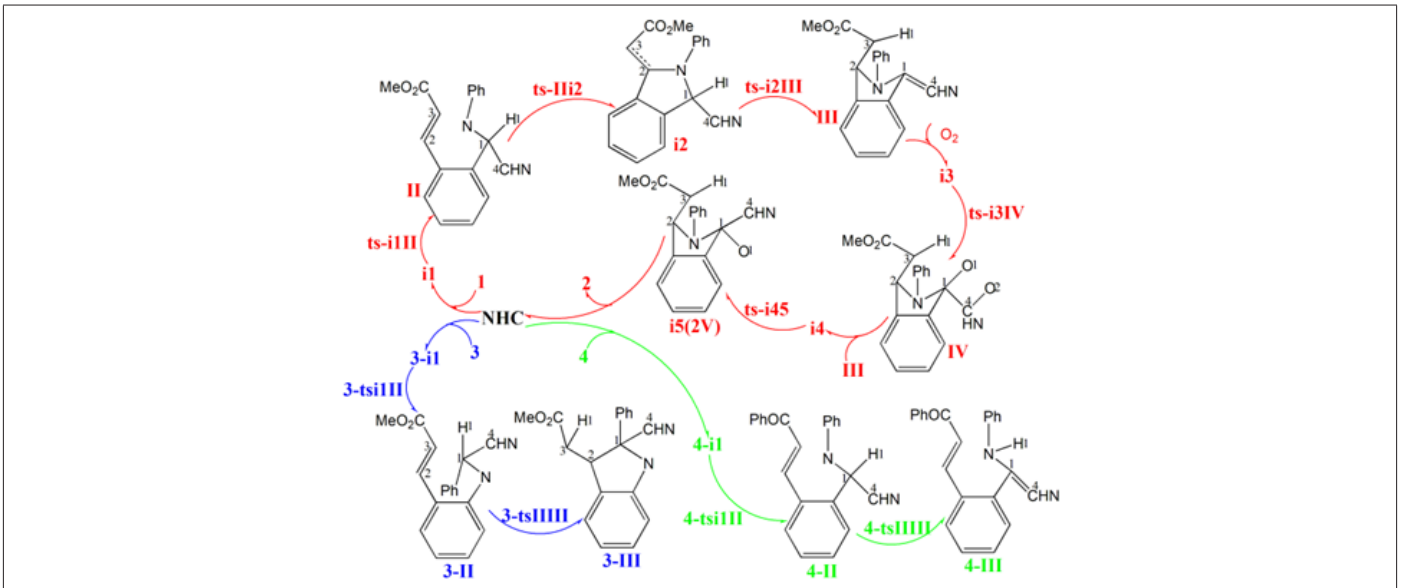

Scheme 2: Proposed reaction mechanism of N-heterocyclic carbene-catalyzed tandem imine umpolung-cyclization of aldimine 1, imine derivative 3, 4. TS is named according to the two intermediates it connects.

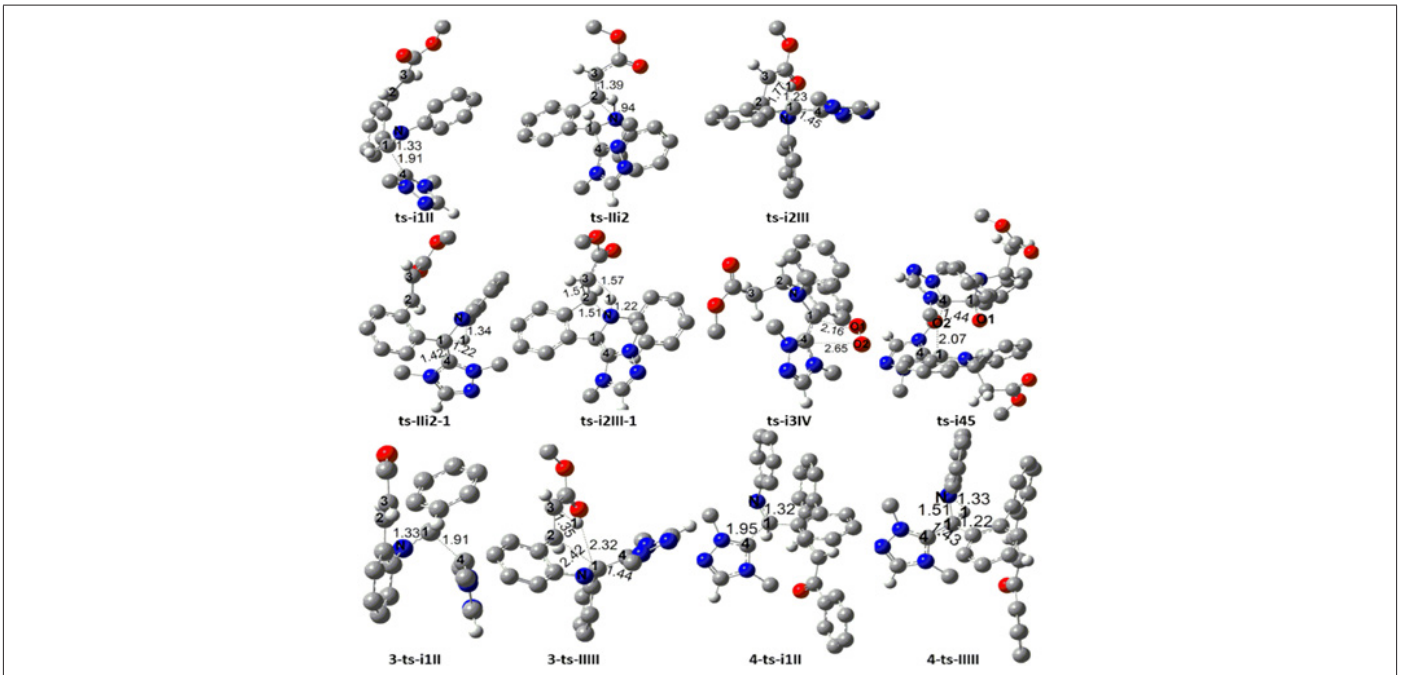

Figure 1: Geometric structures of TSs for N-heterocyclic carbene-catalyzed tandem imine umpolung-cyclization. Selected bond distances are given in Å. Irrelevant hydrogen atoms are omitted for clarity.
Figure 1a:

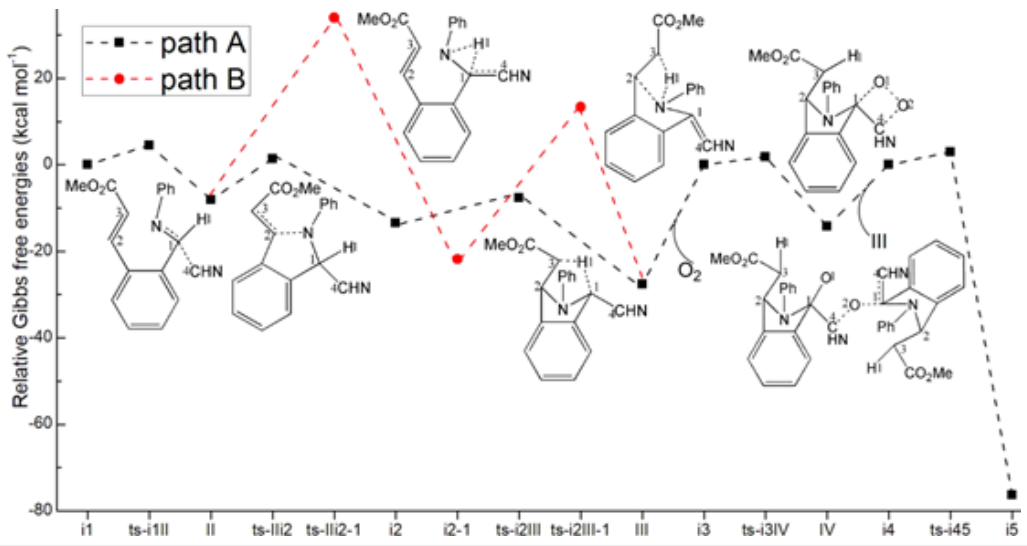

Figure 1b:

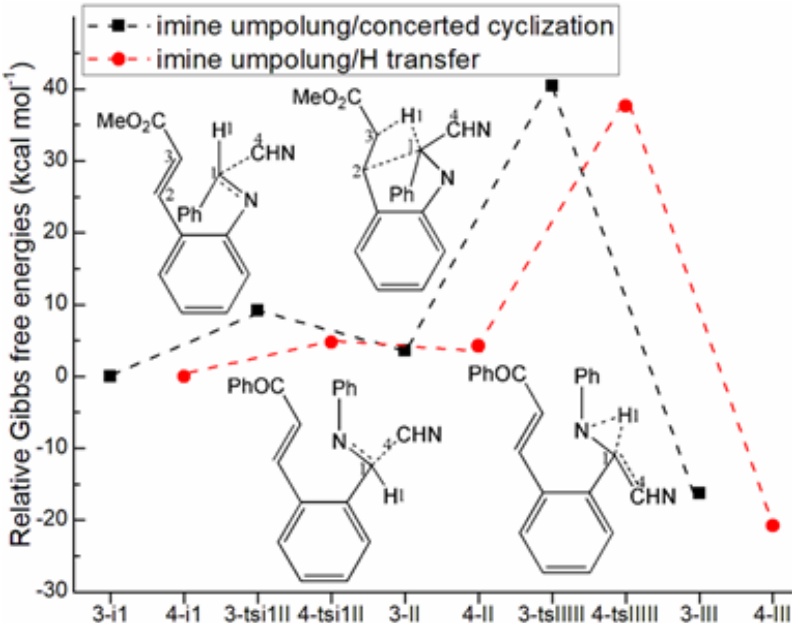

Figure 2: Relative Gibbs free energy profile of N-heterocyclic carbene-catalyzed tandem imine umpolung-cyclization in solvent phase starting from complex (a) i1, i3, i4 (b) 3-i1, 4-i1.

Table 1: The activation energy (in kcal mol^{-1}) of all reactions in gas and solvent.

TS	$\Delta G^{\neq}_{gas}$	$\Delta G^{\neq}_{sol}$
ts-i1II	15.0	4.5
ts-IIi2	18.7	9.4
ts-i2III	15.5	5.7
ts-IIi2-1	42.9	42.0
ts-i2III-1	40.2	35.1
ts-i3IV	3.7	1.9
ts-i45	14.4	3.0
3-tsi1II	10.9	9.1
3-tsIII II	40.4	36.8
4-tsi1II	10.1	4.8
4-tsIII II	39.7	33.4

Imine Umpolung-aza-Michael Addition-H Transfer

A complex i1 between 1 and NHC was taken as starting point of initial imine umpolung, where the nucleophilic addition of NHC proceeds via ts-i1II with a activation energy of 4.5kcal mol-1 exothermic by -8.1kcal mol^{-1} furnishing tetrahedral intermediate II. The transition vector corresponds to the approaching of C1 to C4 and elongation of C1-N double bond (1.91, 1.33 Å) (Figure S1a). This step 1 is fairly easy whether from small barrier kinetically or from heat release thermodynamically. The sp2 imine C1 becomes sp3 involving C1-C4 single bond with lone pair located C4 of NHC. To highlight the idea of changes both in electron density and mo-

lecular orbital interactions responsible for the reactivity of organic molecules, quantum chemical tool Multiwfn was applied to analyze of electron density such as MBO results of bonding atoms and contribution of atomic orbital to HOMO of typical TSs (Table 2,3). HOMO distribution was presented by Figure 3. For ts-i1II, HOMO is mainly contributed by the big π orbital of aromatic imine benzene ring, bonding π orbital of C1-N and lone pair electron on C4 (2.41%, 30.27%, 9.71%). MBO values of C1···C4 and C1···N (0.50, 1.41) suggest the bond formation and weaken of double bond.

Table 2: Contribution (%) of Natural Atomic Orbital (NAO) to Highest Occupied Molecular Orbital (HOMO) of typical TSs.

	C1	C4	N	
ts-i1II HOMO	2.41	9.71	30.27	
	N	C2	C3	
ts-IIi2 HOMO	22.45	1.22	39.85	
	C1	C3	O	
ts-i2III HOMO	9.35	54.29	14.01	
	C1	C4	N	
ts-IIi2-1 HOMO	11.92	2.85	31.46	
	N	C3		
ts-i2III-1 HOMO	4.62	7.49		
	C1	C4	O1	O2
ts-i3IV HOMO	21.5	1.82	7.31	11.37
	C1	C3	C2	N
3-tsIII II HOMO	9.06	23.93	13.49	17.03
	C1	N	C4	
4-tsIII II HOMO	13.47	32.74	3.06	

Table 3: Mayer Bond Order (MBO) of typical TSs.

	C1···C4	C1···N	
ts-i1II	0.5	1.41	
	N···C2	C2···C3	
ts-IIi2	0.39	1.42	
	C1···H1	H1···C3	C1···C4
ts-i2III	0.61	0.28	1.21
	C1···H1	H1···N	C1···C4
ts-IIi2-1	0.51	0.29	1.26
	N···C2	N···H1	H1···C3
ts-i2III-1	0.78	0.43	0.41
	C1···C4	C1···O1	O1···O2
ts-i3IV	1.23	0.3	1.4
	C1···C2	H1···C3	C1···N
3-tsIIIII	0.28	0.34	1.19
	C1···H1	H1···N	C1···C4
4-tsII III	0.5	0.28	1.13

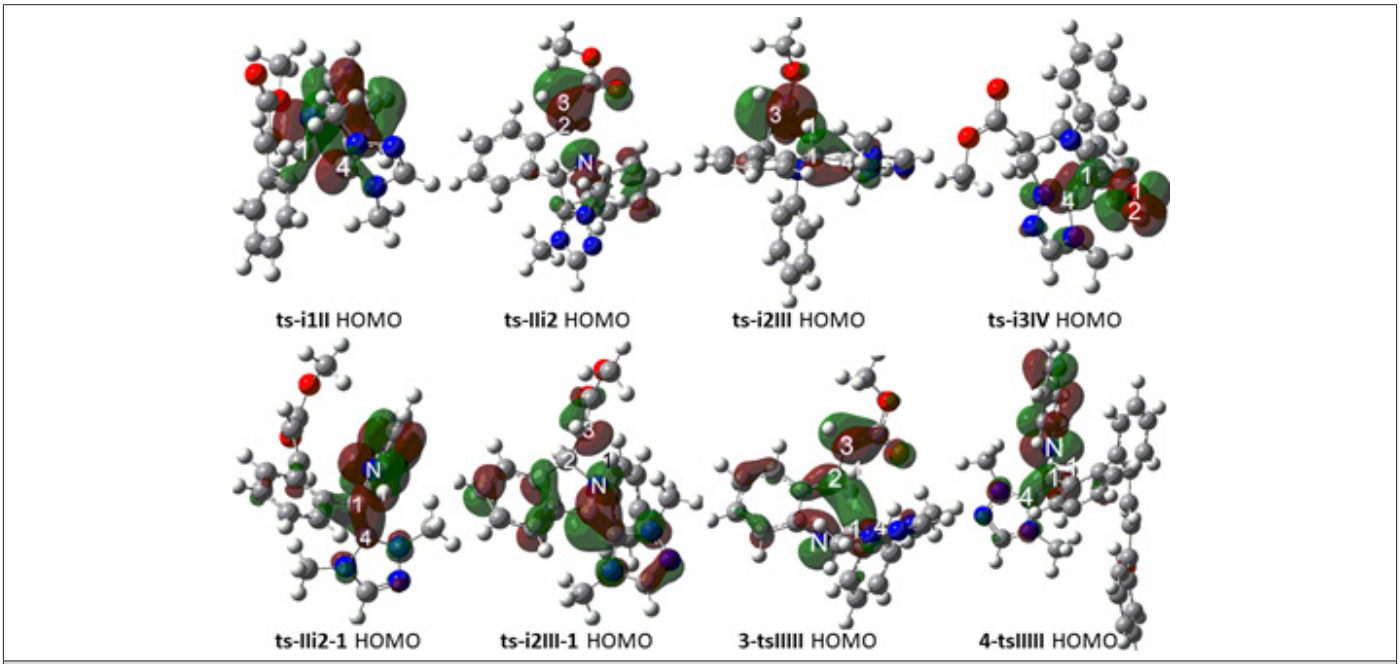

Figure 3: Highest Occupied Molecular Orbital (HOMO) of typical TSs. Different colors are used to identify the phase of the wave functions.

Subsequently, the intramolecular aza-Michael addition takes place via ts-IIi2 as step 2 with a activation energy of 9.4 kcal mol^{-1} leading to i2 exothermic by -13.4 kcal mol^{-1}. The transition vector of ts-IIi2 includes the link of nucleophilic N to C2 and stretching of C2-C3 double bond (1.94, 1.39 Å) (Figure S1b). Owing to the electron withdrawing ester CO_2Me, C2 is more positive suitable for being nucleophilic attack, which turns to be sp3 hybrid with new N-C2 single bond. In resultant i2, the conjugation moves from alkene C2-C3 to C3 and ester group. This situation is verified by HOMO of ts-IIi2 major on bonding π orbital between C3 and CO_2Me, lone pair p orbital of N, while minor on C2 (22.45%, 39.85%, 1.22%). MBO values of N···C2 and C2···C3 (0.39, 1.42) also confirms this changing tendency.

With more π electron, C3 is ready for the following proton transfer thereby easy to accept H1 from C1. Via ts-i2III, the activation energy of step 3 is 5.7 kcal mol^{-1} with respect to i2 forming aza-Breslow intermediate III continuously exothermic by -27.7 kcal mol^{-1}. The transition vector of ts-i2III corresponds to H1 transfer from C1 to C3 and contraction of C1-C4 single bond to double (1.23, 1.77, 1.45 Å) (Figure S1c). Characterized by typical C1-C4 double bond linking with NHC and sp3 type C2, C3, the structure of III is more stable than II or i2 as a powerful driving force in thermodynamics. Clearly, these three steps are quite readily accessible along with small activation energy in kinetics. The correctness of ts-i2III can also be approved by HOMO mainly consisting of p orbital on C3 beneficial to accept proton minor on bonding π orbital of C1-C4 denoting the upcoming double bond (54.29%, 9.35%). What's more, MBO values of C1···H1, H1···C3 and C1···C4 (0.61, 0.28, 1.21) echo the evolution process.

Alternative H Transfer-Concerted aza-Michael Addition

An alternative structure of i2 is located denoted as i2-1 with lower relative energy of -21.8 kcal mol^{-1}. So from II to III, another path B via i2-1 is also possible (red dash line of Figure 1a). A simple proton transfer occurs at first via ts-IIi2-1, the transition vector of which is about H1 shifting from C1 to N and the consequent shortening of C1-C4 single bond to double (1.22, 1.34, 1.42 Å). Once imine N becomes nonequivalent sp3 hybridization, i2-1 is actually already an aza-Breslow intermediate linking NHC therefore more stable than i2.

Like a transfer station, H1 is provided by N to C3 in the following step. This enhances the nucleophilic ability of N thus initiates the concerted aza-Michael addition. That is N-C2 bonding via ts-i2III-1 with activation energy of 35.1 kcal mol^{-1} relative to $i2^{-1}$ affording cyclization product III. The transition vector of ts-i2III-1 consists of H1 moving from N to C3, closing of N to C2 and the elongation of C2-C3 double bond to single (1.22, 1.57, 1.51, 1.51 Å).

The validity of ts-IIi2-1 and ts-i2III-1 is verified by their HOMO composition. The former is mainly on lone pair p orbital of N ready to accept proton and minor on bonding π orbital of upcoming C1-C4 double bond (31.46%, 11.92%, 2.85%). In agreement with this, MBO values of C1···H1, H1···N and C1···C4 are 0.51, 0.29, 1.26. For the latter, a major disperse distribution on benzene ring and NHC heterocyclic ring is seen together with minor on p orbital of N, C3 (4.62%, 7.49%) while almost none on C2. MBO values of N···C2 and N···H1···C3 (0.78, 0.43, 0.41) are also in accordance with this. Although path B seems to be reasonable and existing parallel with path A, the activation energy of ts-IIi2-1 high to be 42.0kcal mol-1 makes it impossible.

Duplicate Oxidation and Intermolecular Oxygen Exchange

With oxygen in air as oxidant, one molecular is added to III forming a complex i3 taken as the starting point of process in the following step 4. Two sp2 type C1 and C4 are both oxidized via ts-i3IV with a small barrier of 1.9kcal mol^{-1} exothermic by -14.2kcal mol^{-1} giving stable intermediate IV with C1-O1 and C4-O2 two single bonds. However, the structure IV proposed in experiment via so called radical recombination was not located showing that two O atoms cannot remain linked once O_2 molecule is connected to carbon. The transition vector of ts-i3IV demonstrates simultaneous closing of O1 to C1, O2 to C4 and cleavage of O1-O2, stretching C1-C4 double bond to single (2.16, 2.65 Å). Homo consists of C1-C4 bonding π orbital and O1-O2 anti-bonding π orbital (21.50%, 7.31%, 11.37%). MBO values denote the upcoming C1···O1 single bond and still double C1···C4 and O1···O2 connection (0.30, 1.23, 1.40).

The step 5 is the reaction initiated from a complex binding intermediate IV and III denoted as i4. This intermolecular oxygen exchange proceeds via ts-i45 also with a small barrier of 3.0 kcal mol^{-1} greatly exothermic by -76.3 kcal mol^{-1}. As is described by transition vector of ts-i45 (Figure S1d), O2 is given by C4 of IV to oxidize C1 of III (1.44, 2.07 Å) yielding i5, which is a binary complex of intermediate V. The desired N-aryl 3-isoindolinone 2 is produced after expulsion of NHC from V. From the perspective of overall five steps, the intramolecular aza-Michael addition of step 2 is determined to be rate-limiting of path A kinetically.

Breslow Intermediate of Substrates 3, 4 and Solvent Effect

For imine derivative 3 as substrate, the complex 3-i1 between it and NHC is taken as starting point of previous two steps affording Breslow intermediate. Via 3-tsi1II, the activation energy of imine umpolung in step 1 is 9.1 kcal mol^{-1} obtaining 3-II endoergic by 3.6 kcal mol^{-1}, from which a concerted step of cyclization is required via 3-tsIII II to furnish aza-Breslow 3-III. The activation energy of step 2 is increased to be 36.8 kcal mol^{-1} determined as rate-limiting. The transition vector of 3-tsi1II is about nucleophilic attack of C4 to C1 and stretching of C1-N (1.91, 1.33 Å). In the structure of 3-II, NHC is linked to imine C1 via C1-C4 single bond. Then H1 shifts from sp3 hybrid C1 to sp2 type C3 illustrated by transition vector of 3-tsII III (Figure S1e). The transient sp2 state of C1 is not stable with improved nucleophilic ability inducing its concerted Michael addition to C2. This vibration mode seems like the case of ts-i2III-1. Yet, the cyclization product 3-III is not a typical Breslow intermediate owing to the final elongation of C1-C4 double bond to single (2.32, 1.35, 2.42, 1.44 Å). Homo of 3-tsII III is composed by anti-bonding π orbital of C2-C3, diffuse σ orbital of C1-C2, p orbital of N among C1 and C2 (23.93%, 13.49%, 9.06%, 17.03%). MBO values of C1···C2 and H1···C3 (0.28, 0.34) suggests the cyclization and evident H shift.

When the imine derivative 4 participates in reaction, the starting point is complex denoted as 4-i1. The step 1 of imine umpolung proceeds via 4-tsi1II with the activation energy of 4.8 kcal mol^{-1} endoergic by 4.2 kcal mol^{-1} affording 4-II, from which one step of simple H transfer is required via 4-tsII III to yield aza-Breslow 4-III. The step 2 is also rate-limiting with increased activation energy to be 33.4 kcal mol^{-1}. The nucleophilic attack of C4 to C1 can be seen from transition vector of 4-tsi1II also involving elongation of C1-N double bond (1.95, 1.32 Å). C1-C4 single bond is formed linking NHC to imine C1 in resultant 4-II. Shown by the transition vector of 4-tsII III (Figure S1f), the shift of H1 from sp3 hybrid C1 to sp2 type N (1.22, 1.33 Å) directly gives typical Breslow intermediate 4-III with C1-C4 double bond connecting NHC. Homo of 4-tsII III

is major on lone pair p orbital of N to accept proton and minor on bonding π orbital of C1-C4 indicating upcoming formation of double bond (32.74%, 13.47%). This is matched with MBO values of C1···H1, H1···N and C1···C4 (0.50, 0.28, 1.13).

The impact of DMSO solution is studied in view of the solvent effect on reaction estimated by our approach [32-34]. Obviously, the absolute energies of all stationary points in solution are lower than those in gas phase (Table S1). For the case of 1 as substrate, it is noticed that the oxidation enhances the influence of solvent with relative energies decreased by -70∼-100 kcal mol^{-1} compared with previous process of imine umpolung and intramolecular aza-Michael addition forming III (-40∼-60 kcal mol^{-1}). The effect becomes a little weaker when the substrate is changed to be 3 and 4 (-30∼-40 kcal mol^{-1} vs -40∼-60 kcal mol^{-1}). For most steps, the activation energies are reduced in solution phase compared with in gas (Table S2). With reduction values -9∼-11 kcal mol^{-1}, the solvent effect with substrate 1 (-9.8, -10.4 kcal mol^{-1}) is more visible than imine derivative 3 (-1.7, -3.6 kcal mol^{-1}) or 4 (-5.3, -6.9 kcal mol^{-1}) on generation of Breslow intermediate. Accordingly, the DMSO solution produces favorable influence on this NHC-catalyzed tandem imine umpolung-cyclization of aldimine leading to isoindolinone and other two imine derivatives.

Conclusions

Our DFT calculations provide the first theoretical investigation on tandem imine umpolung-cyclization of aldimine leading to isoindolinone and other two imine derivatives catalyzed by N-heterocyclic carbene. The aldimine was attacked by nucleophilic NHC generating tetrahedral intermediate, the intramolecular aza-Michael addition of which followed by H transfer gives key aza-Breslow intermediate. After oxidation by oxygen molecule, an oxygen atom transfers from its oxidation product to itself affording the complex as precursor of desired N-aryl 3-isoindolinone. Although an alternative path is plausible involving H transfer ahead of concerted aza-Michael addition, it is excluded owing to high activation energy. The preferential path is both favored by thermodynamics and kinetics.

Based on the comparison with other two imine derivatives, the initial step of imine umpolung is consistent for them via nucleophilic addition of NHC. The following intramolecular aza-Michael addition is rate-limiting step. The typical Breslow intermediate is just not available through H transfer concertedly with intramolecular cyclization. The positive solvation effect is suggested by decreased absolute and activation energies in DMSO solution compared with in gas. These results are supported by Multiwfn analysis on FMO composition of specific TSs, and MBO value of vital bonding, breaking.

Supplementary Information

The supporting information includes computation information and cartesian coordinates of stationary points; calculated relative energies for the ZPE-corrected Gibbs free energies (ΔGgas), and Gibbs free energies (ΔGsol) for all species in solution phase at 298 K.

Declarations

Funding

This work was supported by National Natural Science Foundation of China (21973056, 21972079) and Natural Science Foundation of Shandong Province (ZR2019MB050).

Data Availability

Enquiries about data availability should be directed to the authors.

References

1. K Speck, T Magauer (2013) The Chemistry of Isoindolinone Natural Products. Beilstein J Org Chem 9: 2048-2078.
2. HA Blair (2020) Lenalidomide: A Review in Previously Treated Follicular Lymphoma. Drugs 80(13): 1337-1344.
3. SM Evans, RW Foltin, FR Levin, MW Fischman (1995) Behavioral and Subjective Effects of DN-2327 (Pazinaclone) and Alprazolam in Normal Volunteers. Behav Pharmacol 6: 176-186.
4. N Kanamitsu, T Osaki, Y Itsuji, M Yoshimura, H Tsujimoto, M Soga (2007) Novel Water-Soluble Sedative-Hypnotic Agents: Isoindolin-1-one Derivatives. Chem Pharm Bull 55(12): 1682-1688.
5. T Nishiyama, S Chiba, Y Yamada (2008) Antinociceptive Property of Intrathecal and Intraperitoneal Administration of Novel Water-soluble Isoindolin-1-one Derivative, JM 1232 (-) in Rats. Eur J Pharmacol 596(1-3): 56-61.
6. P Thapa, E Corral, S Sardar, BS Pierce, FW Foss Jr (2019) Isoindolinone Synthesis: Selective Dioxane-Mediated Aerobic Oxidation of Isoindolines, J Org Chem 84: 1025-1034.
7. Y Krishna, F Tanaka (2021) Intramolecular Formal [4 + 2] Cycloadditions: Synthesis of Spiro Isoindolinone Derivatives and Related Molecules, Org Lett 23(5): 1874-1879.
8. YM Zhu, Y Fang, H Li, XP Xu, SJ Ji (2021) Divergent Reaction of Isocyanides with o-Bromobenzaldehydes: Synthesis of Ketenimines and Lactams with Isoindolinone Cores, Org Lett 23(19): 7342-7347.
9. AK Mailyan, G Mata, DH Miles, EU Sharif, MR Leleti, et al. (2022) Development of a Robust and Scalable Synthetic Route for a Potent and Selective Isoindolinone PI3Kγ Inhibitor, Organic Process Research & Development 26: 2915-2925.
10. RA Unhale, MM Sadhu, VK Singh (2022) Chiral Brønsted Acid Catalyzed Enantioselective Synthesis of Spiro-Isoindolinone-Indolines via Formal [3+2] Cycloaddition, Org Lett 24(18): 3319-3324.
11. D Enders, O Niemeier, A Henseler (2007) Organocatalysis by N-Heterocyclic Carbenes. Chem Rev 107(12): 5606-5655.
12. DA DiRocco, KM Oberg, T Rovis (2012) Isolable Analogues of the Breslow Intermediate Derived from Chiral Triazolylidene Carbenes. J Am Chem Soc 134(14): 6143-6145.
13. S Lebrun, R Sallio, M Dubois, F Agbossou Niedercorn, E Deniau, et al. (2015) Chiral Phase-Transfer-catalyzed Intra-molecular Aza-Michael Reactions for the Asymmetric Synthesis of Isoindolinones. Eur J Org Chem 2015: 1995-2004.
14. SK Ray, MM Sadhu, RG Biswas, RA Unhale, VK Singh (2019) A General Catalytic Route to Enantioenriched Isoindolinones and Phthalides: Application in the Synthesis of (S)-PD 172938. Org Lett 21: 417-422.
15. M Kumar, S Verma, AK Verma (2020) Ru (II)-Catalyzed Oxidative Olefination of Benzamides: Switchable Aza-Michael and Aza-Wacker Reaction for Synthesis of Isoindolinones. Org Lett 22(12): 4620-4626.
16. R Savela, C Mendez Galvez (2021) Isoindolinone Synthesis via One-Pot

Type Transition Metal Catalyzed C-C Bond Forming Reactions. Chemistry 27(17): 5344-5378.

17. A Patra, S Mukherjee, TK Das, S Jain, RG Gonnade, et al. (2017) N-Heterocyclic-Carbene-Catalyzed Umpolung of Imines. Angew Chem Int Ed 56(10): 2730-2734.

18. JEM Fernando, Y Nakano, C Zhang, DW Lupton (2019) Enantioselective N-Heterocyclic Carbene Catalysis that Exploits Imine Umpolung. Angew Chem Int Ed 58(12): 4007-4011.

19. TK Das, AT Biju (2020) Imines as Acceptors and Donors in N-heterocyclic Carbene (NHC) Organo-catalysis. Chem Commun 56: 8537-8552.

20. X Yang, Y Xie, J Xu, S Ren, B Mondal, et al. (2021) Carbene-Catalyzed Activation of Remote Nitrogen Atoms of (Benz)imidazole-Derived Aldimines for Enantioselective Synthesis of Heterocycles. Angew Chem Int Ed 60(14): 7906-7912.

21. G Wang, QC Zhang, C Wei, Y Zhang, L Zhang, et al. (2021) Asymmetric Carbene-Catalyzed Oxidation of Functionalized Aldimines as 1,4-Dipoles. Angew Chem Int Ed 60(14): 7913-7919.

22. Satyam K, Harish B, Nanubolu JB, Suresh S (2020) N-Heterocyclic Carbene (NHC)-Catalyzed Tandem Imine Umpolung-Aza-Michael Addition-Oxidation of β-Carboline Cyclic Imines. Chem Commun 56(18): 2803-2806.

23. Ramarao J, Yadav S, Satyam K, Suresh S (2020) N-Heterocyclic Carbene (NHC)-Catalyzed Oxidation of Unactivated Aldimines to Amides via Imine Umpolung under Aerobic Conditions. RSC Adv 12(13): 7621-7625.

24. Yadav S, Nanubolu JB, Suresh S (2022) Sequential One-Pot Carbene-Catalyzed Intramolecular Stetter Reaction and Acid-Mediated Condensation: Access to Heteroatom Analogues of π-Extended Polyaromatic Hydrocarbons. Org Lett 24(38): 6930-6935.

25. Ramarao J, Behera PC, Reddy MS, Suresh S (2024) Carbene-Catalyzed Tandem Imine Umpolung–Intramolecular Aza Conjugate Addition–Oxidation to Access N-Substituted Isoindolinones. J Org Chem 89: 414-424.

26. Frisch MJ, Trucks GW, Schlegel HB, Scuseria GE, Robb MA, et al. (2017) The Effects of Oxidation States, Spin States and Solvents on Molecular Structure, Stability and Spectroscopic Properties of Fe-Catechol Complexes: A Theoretical Study 7.

27. Stephens PJ, Devlin FJ, Chabalowski CF, Frisch MJ (1995) Ab initio Calculation of Vibrational Absorption and Circular Dichroism Spectra Using Density Functional Force Fields. J Phys Chem 98: 11623.

28. Becke AD (1996) Density-functional thermochemistry. IV. A new dynamical correlation functional and implications for exact-exchange mixing, J Chem Phys 104: 1040-1046.

29. Lee CT, Yang WT, Parr RG (1998) Development of the Colle-Salvetti correlation-energy formula into a functional of the electron density. Phys Rev B Condens Matter 37(2): 785-789.

30. Li X, Kong X, Yang S, Meng M, Zhan X, et al. (2019) Bifunctional Thiourea-Catalyzed Asymmetric Inverse-Electron-Demand Diels-Alder Reaction of Allyl Ketones and Vinyl 1,2-Diketones via Dienolate Intermediate. Org Lett 21(7): 1979-1983.

31. Krenske EH, Houk KN, Harmata M (2015) Computational Analysis of the Stereochemical Outcome in the Imidazolidinone-Catalyzed Enantioselective (4 + 3)-Cycloaddition Reaction. J Org Chem 80(2): 744-750.

32. Lv H, Han F, Wang N, Lu N, Song Z, et al. (2022) Ionic Liquid Catalyzed C-C Bond Formation for the Synthesis of Polysubstituted Olefins, Eur. J Org Chem e202201222.

33. Zhuang H, Lu N, Ji N, Han F, Miao C (2021) Bu4NHSO4-Catalyzed Direct N-Allylation of Pyrazole and its Derivatives with Allylic Alcohols in Water: A Metal-free, Recyclable and Sustainable System. Adv Synth Catal 363: 5461-5472.

34. Lu N, Liang H, Qian P, Lan X, Miao C (2020) Theoretical investigation on the mechanism and enantioselectivity of organocatalytic asymmetric Povarov reactions of anilines and aldehydes. Int J Quantum Chem e26574.

35. Tapia O (1992) Solvent effect theories: Quantum and classical formalisms and their applications in chemistry and biochemistry. J Math Chem 10(1): 139-181.

36. Tomasi J, Persico M (1994) Molecular Interactions in Solution: An Overview of Methods Based on Continuous Distributions of the Solvent. Chem Rev 94 (7): 2027-2094.

37. Simkin BY, Sheikhet I (1995) Quantum Chemical and Statistical Theory of Solutions-A Computational Approach, Ellis Horwood, London.

38. Tomasi J, Mennucci B, Cammi R (2005) Quantum Mechanical Continuum Solvation Models. Chem Rev 105(8): 2999-3093.

39. Marenich AV, Cramer CJ, Truhlar DG (2009) Universal solvation model based on solute electron density and on a continuum model of the solvent defined by the bulk dielectric constant and atomic surface tensions, J Phys Chem B 113(18): 6378-6396.

40. Reed AE, Weinstock RB, Weinhold F (1985) Natural population analysis. J Chem Phys 83(2): 735-746.

41. Reed AE, Curtiss LA, Weinhold F (1988) Intermolecular interactions from a natural bond orbital donor-acceptor viewpoint. Chem Rev 88(6): 899-926.

42. Foresman JB, Frisch A (1996) Exploring Chemistry with Electronic Structure Methods. 2nd ed., Gaussian, Inc., Pittsburgh.

43. Lu T, Chen F (2012) Multiwfn: A multifunctional wavefunction analyzer. J Comput Chem 33(5): 580-592.

Supplementary Information

Theoretical Investigation on N-Heterocyclic Carbene-Catalyzed Tandem Imine Umpolung-Cyclization via Breslow Intermediate

Nan Lu*, Chengxia Miao and Xiaozheng Lan

College of Chemistry and Material Science, Shandong Agricultural University, Taian, China.

Table of Contents **Pages**

Software: GAUSSIAN09

Level of Theory: M06-2X

Basis Set: 6-31G(d)

Geometry [Cartesian coordinates]:

Optimized Cartesian coordinates for ts-i1II

Center Number	Atomic Number	Atomic Type	Coordinates (Angstroms) X	Y	Z
1	6	0	-3.300060	0.262809	0.632027
2	6	0	-3.334191	-1.064396	1.052024
3	6	0	-2.164292	-1.669280	1.495709
4	6	0	-0.943974	-0.988891	1.525006
5	6	0	-0.919484	0.371481	1.153236
6	6	0	-2.105383	0.966183	0.696512
7	6	0	0.275661	-1.697373	2.103919
8	6	0	0.289615	1.213962	1.250860
9	6	0	0.661624	2.080986	0.304545
10	6	0	1.930305	2.824848	0.461637
11	8	0	2.616101	2.857730	1.456789
12	8	0	2.256985	3.465804	-0.678524
13	6	0	3.518550	4.121813	-0.642220
14	6	0	0.222972	-3.493562	1.471256
15	6	0	2.055378	-0.958301	0.737184
16	6	0	1.440433	-1.198578	-0.507596
17	6	0	2.023576	-0.766527	-1.695668
18	6	0	3.241350	-0.094704	-1.688710
19	6	0	3.876471	0.130422	-0.464010
20	6	0	3.301386	-0.298394	0.721058
21	7	0	0.021435	-4.147553	0.294074
22	6	0	0.779167	-5.289524	0.299634
23	7	0	1.442899	-5.405403	1.407119
24	7	0	1.085204	-4.296998	2.108715
25	6	0	1.720870	-4.033755	3.393612
26	6	0	-0.846749	-3.758786	-0.810294
27	1	0	-4.202689	0.753738	0.281818
28	1	0	-4.265291	-1.623067	1.041099
29	1	0	-2.184466	-2.707389	1.823424
30	1	0	-2.078911	2.016449	0.420940

31	1	0	0.933839	1.092339	2.118434
32	1	0	0.043631	-1.975824	3.140337
33	1	0	0.129811	2.192381	-0.635526
34	1	0	3.641891	4.589118	-1.618537
35	1	0	4.314436	3.395046	-0.459982
36	1	0	3.540267	4.872891	0.151172
37	1	0	0.459986	-1.658373	-0.539902
38	1	0	1.509248	-0.945073	-2.637370
39	1	0	3.688665	0.248826	-2.616026
40	1	0	4.829674	0.652415	-0.434472
41	1	0	3.776846	-0.102992	1.677251
42	1	0	0.814109	-5.992541	-0.519838
43	1	0	2.488059	-4.793969	3.527597
44	1	0	0.984576	-4.104260	4.196738
45	1	0	2.157319	-3.030814	3.348836
46	1	0	-1.514353	-4.588661	-1.052584
47	1	0	-0.241153	-3.501376	-1.681882
48	1	0	-1.437029	-2.894854	-0.509404
49	7	0	1.543287	-1.300782	1.977465

Optimized Cartesian coordinates for ts-IIi2

Center Number	Atomic Number	Atomic Type	Coordinates (Angstroms) X	Y	Z
1	6	0	0.972758	3.830248	-1.558904
2	6	0	-0.126536	4.075415	-0.739161
3	6	0	-0.641767	3.052816	0.057346
4	6	0	-0.075389	1.783505	-0.007986
5	6	0	1.062661	1.545057	-0.785151
6	6	0	1.582406	2.576640	-1.562467
7	6	0	-0.379536	0.540495	0.814447
8	6	0	1.732067	0.211731	-0.608611
9	6	0	2.865966	0.174286	0.195043
10	6	0	3.570325	-1.081517	0.248697
11	8	0	3.217812	-2.103243	-0.315510
12	8	0	4.728542	-1.161588	0.989220

13	6	0	5.263192	0.009916	1.559687
14	6	0	-1.760698	0.214595	1.318997
15	6	0	-0.533704	-1.226695	-0.856836
16	6	0	-1.528944	-0.614028	-1.638629
17	6	0	-2.167985	-1.306146	-2.666795
18	6	0	-1.808227	-2.614366	-2.966530
19	6	0	-0.770851	-3.210727	-2.243872
20	6	0	-0.139987	-2.533198	-1.211739
21	7	0	-3.025601	0.542107	0.964527
22	6	0	-3.859693	-0.198077	1.761388
23	7	0	-3.196134	-0.952311	2.581119
24	7	0	-1.903475	-0.687673	2.296407
25	6	0	-0.828135	-1.406216	2.978629
26	6	0	-3.530993	1.422445	-0.090225
27	1	0	1.374474	4.627999	-2.176163
28	1	0	-0.573076	5.064524	-0.705834
29	1	0	-1.465531	3.261443	0.738678
30	1	0	2.476126	2.395639	-2.152466
31	1	0	1.717615	-0.481743	-1.450107
32	1	0	0.198916	0.674440	1.747180
33	1	0	3.091649	0.997908	0.860900
34	1	0	6.237980	-0.264860	1.967863
35	1	0	4.634691	0.392614	2.374268
36	1	0	5.392970	0.801133	0.812613
37	1	0	-1.752667	0.436111	-1.490751
38	1	0	-2.934894	-0.804153	-3.252760
39	1	0	-2.304640	-3.153022	-3.767376
40	1	0	-0.449966	-4.218514	-2.492320
41	1	0	0.690729	-2.969704	-0.663290
42	1	0	-4.936401	-0.147918	1.694056
43	1	0	-1.259815	-2.332060	3.353948
44	1	0	-0.452216	-0.804101	3.808644
45	1	0	-0.046421	-1.600062	2.237022
46	1	0	-3.986050	0.809448	-0.869910
47	1	0	-2.713050	1.998631	-0.512273
48	1	0	-4.268125	2.098011	0.347794
49	7	0	0.178821	-0.636435	0.188892

Optimized Cartesian coordinates for ts-i2III

Center Number	Atomic Number	Atomic Type	Coordinates (Angstroms) X	Y	Z
1	6	0	-0.166454	4.240529	0.960618
2	6	0	-0.595707	3.562115	2.093507
3	6	0	-0.542093	2.163729	2.156346
4	6	0	-0.060429	1.460112	1.063267
5	6	0	0.338626	2.151334	-0.100646
6	6	0	0.303691	3.531455	-0.150919
7	6	0	0.175909	0.001475	0.688033
8	6	0	0.740853	1.126608	-1.162754
9	6	0	2.163496	0.705989	-0.932895
10	6	0	2.612617	-0.405408	-1.705313
11	8	0	1.903234	-1.135130	-2.397872
12	8	0	3.945011	-0.761916	-1.648472
13	6	0	4.825799	0.003427	-0.862751
14	6	0	-0.134985	-1.228170	1.384044
15	6	0	-1.448419	-0.036005	-1.183137
16	6	0	-2.566619	0.019393	-0.345603
17	6	0	-3.849150	-0.074186	-0.886975
18	6	0	-4.033001	-0.212371	-2.257166
19	6	0	-2.916119	-0.272536	-3.093586
20	6	0	-1.636091	-0.198586	-2.565545
21	7	0	-0.121481	-1.467583	2.725249
22	6	0	-0.293710	-2.816689	2.887346
23	7	0	-0.398521	-3.423425	1.751430
24	7	0	-0.288508	-2.440178	0.816618
25	6	0	-0.246952	-2.842470	-0.597902
26	6	0	0.219391	-0.539020	3.794182
27	1	0	-0.219529	5.324395	0.927806
28	1	0	-0.992024	4.116196	2.939072
29	1	0	-0.918126	1.666342	3.043450
30	1	0	0.613901	4.057538	-1.049492
31	1	0	0.466927	1.400549	-2.186251
32	1	0	1.389545	0.012225	0.503514

33	1	0	2.851265	1.467289	-0.587702
34	1	0	5.794202	-0.499376	-0.905859
35	1	0	4.490510	0.060906	0.180404
36	1	0	4.938426	1.023551	-1.250965
37	1	0	-2.439560	0.153973	0.724704
38	1	0	-4.709264	-0.028890	-0.225069
39	1	0	-5.033433	-0.283289	-2.671817
40	1	0	-3.045694	-0.401541	-4.164218
41	1	0	-0.751910	-0.307598	-3.188615
42	1	0	-0.329422	-3.295914	3.854620
43	1	0	-1.190877	-2.579696	-1.077722
44	1	0	-0.119444	-3.923492	-0.578608
45	1	0	0.576179	-2.340092	-1.118613
46	1	0	0.774381	-1.087218	4.556795
47	1	0	-0.680064	-0.108266	4.237277
48	1	0	0.851313	0.252658	3.391444
49	7	0	-0.112081	-0.033695	-0.731892

Optimized Cartesian coordinates for ts-IIi2-1

Center Number	Atomic Number	Atomic Type	Coordinates (Angstroms) X	Y	Z
1	6	0	-3.070008	1.133766	1.875604
2	6	0	-2.821311	-0.109142	2.449571
3	6	0	-1.659059	-0.805121	2.120522
4	6	0	-0.745669	-0.286300	1.200087
5	6	0	-1.011019	0.964563	0.604518
6	6	0	-2.166612	1.662532	0.955484
7	6	0	0.537191	-0.991559	0.918530
8	6	0	-0.108603	1.465974	-0.444126
9	6	0	0.362801	2.707951	-0.561137
10	6	0	1.279323	3.008391	-1.700427
11	8	0	1.158641	2.514116	-2.791664
12	8	0	2.275391	3.893649	-1.476198
13	6	0	2.635668	4.202797	-0.136748
14	6	0	0.532394	-2.247196	0.248380
15	6	0	2.605443	-0.040505	-0.093170

16	6	0	2.406392	-0.559185	-1.390940
17	6	0	3.285633	-0.244623	-2.428345
18	6	0	4.404957	0.545725	-2.212260
19	6	0	4.641016	1.032605	-0.922052
20	6	0	3.772117	0.739189	0.112683
21	7	0	-0.462845	-2.828973	-0.498041
22	6	0	0.024069	-4.033979	-0.937794
23	7	0	1.233035	-4.249675	-0.537044
24	7	0	1.553791	-3.137903	0.185590
25	6	0	2.780730	-3.106724	0.958390
26	6	0	-1.709457	-2.215125	-0.931456
27	1	0	-3.966015	1.688247	2.136092
28	1	0	-3.519000	-0.528686	3.168100
29	1	0	-1.438753	-1.757267	2.598601
30	1	0	-2.370036	2.614215	0.471761
31	1	0	0.232984	0.742030	-1.185238
32	1	0	1.356579	-1.083579	1.823269
33	1	0	0.149081	3.471715	0.182016
34	1	0	3.638391	4.628520	-0.189936
35	1	0	2.655396	3.302747	0.484897
36	1	0	1.955497	4.944214	0.297308
37	1	0	1.536757	-1.167074	-1.621880
38	1	0	3.079342	-0.628828	-3.423470
39	1	0	5.079837	0.783769	-3.027160
40	1	0	5.512439	1.652375	-0.726166
41	1	0	3.940040	1.123312	1.115278
42	1	0	-0.551986	-4.710495	-1.551859
43	1	0	3.332872	-4.008578	0.700008
44	1	0	2.539218	-3.112009	2.027535
45	1	0	3.361902	-2.216868	0.714240
46	1	0	-2.139602	-2.850896	-1.706526
47	1	0	-1.504753	-1.225036	-1.345600
48	1	0	-2.408383	-2.115321	-0.099165
49	7	0	1.752170	-0.110395	0.992011

Optimized Cartesian coordinates for ts-i2III-1

Center	Atomic	Atomic	Coordinates (Angstroms)

Number	Number	Type	X	Y	Z
1	6	0	-3.059305	1.806026	0.241661
2	6	0	-3.261632	0.479173	0.614538
3	6	0	-2.199938	-0.420885	0.687538
4	6	0	-0.911149	0.010924	0.356262
5	6	0	-0.709217	1.368257	0.048625
6	6	0	-1.764796	2.259883	-0.020538
7	6	0	0.369759	-0.676657	0.361003
8	6	0	0.752361	1.691874	-0.014065
9	6	0	1.356813	2.254995	1.252352
10	6	0	2.340314	3.295622	1.069228
11	8	0	2.828070	3.621912	-0.005283
12	8	0	2.839438	3.924058	2.176823
13	6	0	2.379206	3.543691	3.455517
14	6	0	0.708312	-1.946978	0.762145
15	6	0	2.312522	-0.051078	-1.097660
16	6	0	2.148947	-1.197608	-1.869314
17	6	0	3.058979	-1.476904	-2.887553
18	6	0	4.123547	-0.618840	-3.136573
19	6	0	4.273234	0.531835	-2.364577
20	6	0	3.377815	0.821019	-1.341714
21	7	0	-0.057556	-3.102959	0.681135
22	6	0	0.741028	-4.129242	1.144851
23	7	0	1.910359	-3.731224	1.503807
24	7	0	1.909719	-2.380725	1.260437
25	6	0	2.965569	-1.555768	1.811078
26	6	0	-1.164866	-3.299792	-0.242133
27	1	0	-3.898428	2.491630	0.187648
28	1	0	-4.261544	0.137309	0.865159
29	1	0	-2.381160	-1.432303	1.032996
30	1	0	-1.576960	3.305260	-0.249666
31	1	0	1.091413	2.218065	-0.909727
32	1	0	1.944816	0.822803	0.975170
33	1	0	0.690138	2.295335	2.108423
34	1	0	2.994768	4.087343	4.173910
35	1	0	2.492726	2.465318	3.615413
36	1	0	1.328424	3.816995	3.607396

37	1	0	1.310516	-1.860521	-1.691040
38	1	0	2.926034	-2.371625	-3.488183
39	1	0	4.830491	-0.841213	-3.929677
40	1	0	5.092453	1.217273	-2.557134
41	1	0	3.479890	1.738787	-0.763793
42	1	0	0.401292	-5.153663	1.194510
43	1	0	3.630095	-2.222312	2.358775
44	1	0	2.538182	-0.811570	2.491913
45	1	0	3.524243	-1.047112	1.019954
46	1	0	-2.120929	-3.388135	0.277529
47	1	0	-0.986834	-4.207672	-0.823344
48	1	0	-1.203190	-2.441055	-0.916413
49	7	0	1.426181	0.276763	0.014198

Optimized Cartesian coordinates for ts-i3IV

Center Number	Atomic Number	Atomic Type	Coordinates (Angstroms) X	Y	Z
1	6	0	-2.490271	-2.378570	3.647536
2	6	0	-1.167929	-2.794237	3.517147
3	6	0	-0.326545	-2.244797	2.548504
4	6	0	-0.815398	-1.240619	1.710373
5	6	0	-2.164020	-0.874621	1.817942
6	6	0	-3.001494	-1.412689	2.779205
7	6	0	-2.482893	0.154628	0.763736
8	6	0	-2.460873	1.555154	1.398571
9	6	0	-2.847836	2.622009	0.392249
10	8	0	-3.791121	2.488779	-0.342208
11	8	0	-2.125715	3.761368	0.313967
12	6	0	-1.043410	4.015573	1.200116
13	6	0	0.893280	0.347263	0.532969
14	6	0	-1.653357	-0.444280	-1.513405
15	6	0	-0.736400	-1.225253	-2.231214
16	6	0	-1.007339	-1.582227	-3.549014
17	6	0	-2.179739	-1.178896	-4.179999
18	6	0	-3.078422	-0.386764	-3.472536
19	6	0	-2.820181	-0.008169	-2.159646

20	7	0	2.066459	0.231904	1.230700
21	6	0	2.917797	1.193288	0.765479
22	7	0	2.390455	1.892227	-0.181173
23	7	0	1.143849	1.366304	-0.345088
24	6	0	0.337544	1.942524	-1.420474
25	6	0	2.424968	-0.716385	2.272957
26	1	0	-3.130472	-2.826083	4.401246
27	1	0	-0.785946	-3.578458	4.163799
28	1	0	0.673593	-2.634910	2.423150
29	1	0	-4.042375	-1.104970	2.841273
30	1	0	-3.441583	-0.018699	0.273020
31	1	0	-1.475086	1.711287	1.843194
32	1	0	-3.195453	1.594842	2.212547
33	1	0	-0.712581	5.028126	0.970516
34	1	0	-0.212401	3.321227	1.031669
35	1	0	-1.360816	3.968685	2.245979
36	1	0	0.180755	-1.556839	-1.761711
37	1	0	-0.283606	-2.192312	-4.081737
38	1	0	-2.383698	-1.465096	-5.206706
39	1	0	-3.990995	-0.037794	-3.947130
40	1	0	-3.511947	0.657537	-1.655148
41	1	0	3.913792	1.331896	1.158475
42	1	0	0.129853	1.191766	-2.183049
43	1	0	0.951200	2.739590	-1.837460
44	1	0	-0.600280	2.347698	-1.044243
45	1	0	1.685650	-0.696350	3.072460
46	1	0	3.391836	-0.405204	2.671572
47	1	0	2.509994	-1.709170	1.830313
48	6	0	-0.237514	-0.502470	0.554421
49	8	0	1.044008	-2.176500	0.051107
50	8	0	2.177828	-1.899362	-0.419142
51	7	0	-1.370151	0.005671	-0.196661

Optimized Cartesian coordinates for ts-i45

Center	Atomic	Atomic	Coordinates (Angstroms)		
Number	Number	Type	X	Y	Z

1	6	0	1.404950	-4.512467	-0.848558
2	6	0	0.230226	-3.865189	-1.233311
3	6	0	0.134933	-2.481899	-1.088516
4	6	0	1.218355	-1.764877	-0.626137
5	6	0	2.393611	-2.403450	-0.263291
6	6	0	2.493729	-3.786732	-0.352693
7	6	0	3.398545	-1.353606	0.126508
8	6	0	4.801312	-1.659966	-0.403100
9	6	0	5.863859	-0.799508	0.264874
10	8	0	5.995536	-0.787442	1.460084
11	8	0	6.724784	-0.085371	-0.492713
12	6	0	6.537913	0.053438	-1.892544
13	6	0	0.633294	0.589364	-1.599263
14	6	0	3.388972	1.050545	0.121964
15	6	0	3.302157	1.286453	1.500387
16	6	0	3.845398	2.442081	2.053944
17	6	0	4.479676	3.381788	1.244533
18	6	0	4.568116	3.157444	-0.127386
19	6	0	4.028748	1.999160	-0.679449
20	7	0	1.192345	1.947450	-1.558448
21	6	0	1.609308	2.293818	-2.799037
22	7	0	1.585278	1.335484	-3.660538
23	7	0	1.041962	0.269846	-2.974496
24	6	0	1.349998	-1.028608	-3.532888
25	6	0	0.874965	2.888863	-0.524120
26	1	0	1.483199	-5.591622	-0.946923
27	1	0	-0.605835	-4.446518	-1.616434
28	1	0	-0.714884	-1.868742	-1.330936
29	1	0	3.405343	-4.308858	-0.071617
30	1	0	3.455659	-1.282962	1.223942
31	1	0	4.782199	-1.595919	-1.491313
32	1	0	5.062659	-2.689192	-0.130153
33	1	0	7.103279	0.941192	-2.179806
34	1	0	5.488966	0.200233	-2.156202
35	1	0	6.934684	-0.817319	-2.426650
36	1	0	2.774390	0.568947	2.117872
37	1	0	3.772992	2.609652	3.124993
38	1	0	4.908451	4.279533	1.680636

39	1	0	5.060925	3.883454	-0.768502
40	1	0	4.059169	1.827289	-1.751398
41	1	0	1.969578	3.289889	-3.026230
42	1	0	1.706627	-0.847521	-4.547375
43	1	0	0.462437	-1.660360	-3.592073
44	1	0	2.123188	-1.550919	-2.958513
45	1	0	0.935426	3.908735	-0.919955
46	1	0	1.536287	2.785976	0.340226
47	1	0	-0.128799	2.672384	-0.195658
48	6	0	1.284319	-0.254958	-0.410675
49	8	0	0.730664	0.105570	0.739579
50	7	0	2.837771	-0.126925	-0.476297
51	6	0	-1.544428	4.343581	1.535570
52	6	0	-2.068761	4.423683	0.240014
53	6	0	-2.396498	3.272428	-0.464884
54	6	0	-2.241016	2.041712	0.176237
55	6	0	-1.722697	1.960225	1.467507
56	6	0	-1.346759	3.109117	2.150056
57	6	0	-1.701677	0.535294	1.916931
58	6	0	-2.670524	0.315633	3.096929
59	6	0	-2.444648	-1.022861	3.792468
60	8	0	-1.407183	-1.254713	4.349700
61	8	0	-3.404181	-1.971623	3.763350
62	6	0	-4.710647	-1.686269	3.294911
63	6	0	-3.221469	0.444700	-1.534232
64	6	0	-2.217947	-1.587820	0.739103
65	6	0	-1.201245	-2.275195	1.408982
66	6	0	-1.308708	-3.648320	1.570899
67	6	0	-2.391590	-4.343281	1.035615
68	6	0	-3.370079	-3.660661	0.316728
69	6	0	-3.295471	-2.275634	0.177151
70	7	0	-3.114417	-0.318642	-2.647013
71	6	0	-4.024263	0.164307	-3.536821
72	7	0	-4.751091	1.117357	-3.038602
73	7	0	-4.279659	1.250407	-1.780873
74	6	0	-5.090507	2.058978	-0.870788
75	6	0	-2.280973	-1.470481	-2.992618
76	1	0	-1.262143	5.253093	2.055751

77	1	0	-2.167243	5.391690	-0.240704
78	1	0	-2.673776	3.325175	-1.514130
79	1	0	-0.904446	3.045113	3.139916
80	1	0	-0.687080	0.200556	2.127580
81	1	0	-3.697351	0.499030	2.772454
82	1	0	-2.418576	1.072081	3.846985
83	1	0	-5.264610	-2.620051	3.390145
84	1	0	-4.707552	-1.386313	2.242503
85	1	0	-5.194253	-0.915440	3.904507
86	1	0	-0.309837	-1.725172	1.709944
87	1	0	-0.514621	-4.181543	2.083581
88	1	0	-2.465291	-5.418656	1.162993
89	1	0	-4.209500	-4.198855	-0.113525
90	1	0	-4.091384	-1.730834	-0.328125
91	1	0	-4.117623	-0.223394	-4.540227
92	1	0	-6.117600	1.705149	-0.969128
93	1	0	-5.027101	3.111257	-1.146261
94	1	0	-4.735428	1.926837	0.147635
95	1	0	-2.757917	-1.933143	-3.857840
96	1	0	-2.237918	-2.210854	-2.195141
97	1	0	-1.311533	-1.027572	-3.197073
98	6	0	-2.450713	0.673093	-0.295511
99	8	0	-0.809335	0.598561	-1.557497
100	7	0	-2.147980	-0.177717	0.697654

Optimized Cartesian coordinates for 3-tsi1II

Center Number	Atomic Number	Atomic Type	Coordinates (Angstroms) X	Y	Z
1	6	0	-3.397624	0.411148	-0.158503
2	6	0	-3.624161	-0.961227	-0.315804
3	6	0	-2.593937	-1.796580	-0.716804
4	6	0	-1.292989	-1.305477	-0.946982
5	6	0	-1.073677	0.093148	-0.815772
6	6	0	-2.137482	0.922707	-0.427591
7	6	0	0.240143	0.651290	-1.139087
8	6	0	0.737778	1.815243	-0.689474

9	6	0	2.081531	2.244613	-1.152736
10	8	0	2.810273	1.550334	-1.815222
11	8	0	2.518738	3.481764	-0.803370
12	6	0	1.673629	4.386542	-0.116122
13	6	0	1.974582	-2.992409	-0.922331
14	6	0	2.049633	-3.447514	-2.236601
15	6	0	3.175168	-4.145246	-2.670092
16	6	0	4.231161	-4.383889	-1.795181
17	6	0	4.163853	-3.916437	-0.482390
18	6	0	3.039052	-3.223853	-0.050263
19	1	0	-4.206390	1.072924	0.134266
20	1	0	-4.612662	-1.373633	-0.132334
21	1	0	-2.749080	-2.865636	-0.836457
22	1	0	-1.971018	1.995501	-0.372343
23	1	0	0.867697	0.063353	-1.808810
24	1	0	0.180529	2.424396	0.013498
25	1	0	2.223582	5.326708	-0.069385
26	1	0	1.462398	4.048022	0.904226
27	1	0	0.732344	4.549089	-0.651222
28	1	0	1.213578	-3.246461	-2.899306
29	1	0	3.228852	-4.499108	-3.695322
30	1	0	5.108446	-4.927009	-2.133603
31	1	0	4.988070	-4.093343	0.202050
32	1	0	2.968727	-2.871482	0.976813
33	7	0	-0.298258	-2.215679	-1.262197
34	6	0	0.758636	-2.243469	-0.457327
35	1	0	1.023458	-1.356841	0.138494
36	6	0	-1.808935	-3.691056	2.065735
37	7	0	-1.522195	-4.798085	1.454232
38	6	0	0.092557	-3.262780	1.011736
39	7	0	-0.856139	-2.734156	1.831765
40	6	0	0.198578	-5.475123	-0.121033
41	6	0	-0.908745	-1.365819	2.326833
42	1	0	-2.680795	-3.533611	2.683867
43	1	0	-0.040512	-5.138571	-1.134124
44	1	0	-0.269450	-6.436361	0.086352
45	1	0	1.280855	-5.538009	-0.004445
46	1	0	-0.941938	-1.368954	3.418843

47	1	0	-1.789239	-0.860387	1.919520
48	1	0	-0.012277	-0.842470	1.996088
49	7	0	-0.342386	-4.516525	0.827216

Optimized Cartesian coordinates for 3-tsIIIII

Center Number	Atomic Number	Atomic Type	Coordinates (Angstroms) X	Y	Z
1	6	0	-1.609624	4.222389	-0.710323
2	6	0	-0.316080	4.460820	-1.221727
3	6	0	0.627049	3.464003	-1.236778
4	6	0	0.348452	2.167244	-0.714374
5	6	0	-0.945617	1.951611	-0.120563
6	6	0	-1.910737	2.976631	-0.205793
7	6	0	-1.300768	0.661935	0.421552
8	6	0	-2.588180	0.000817	0.096042
9	6	0	-2.926209	-1.200016	0.819825
10	8	0	-2.147241	-1.759410	1.587608
11	8	0	-4.128467	-1.795615	0.607594
12	6	0	-5.088316	-1.152448	-0.208724
13	6	0	1.518083	0.013016	1.161375
14	6	0	2.682917	0.766508	1.385997
15	6	0	3.256644	0.854272	2.647560
16	6	0	2.676637	0.193273	3.728159
17	6	0	1.513719	-0.541061	3.528779
18	6	0	0.932842	-0.626019	2.263833
19	1	0	-2.349867	5.015671	-0.696994
20	1	0	-0.068166	5.440845	-1.620489
21	1	0	1.611807	3.627528	-1.663557
22	1	0	-2.896872	2.778382	0.210749
23	1	0	-0.855549	0.301021	1.332975
24	1	0	-3.197874	0.429281	-0.688503
25	1	0	-5.996005	-1.751727	-0.135590
26	1	0	-4.765487	-1.117502	-1.255689
27	1	0	-5.293876	-0.135403	0.142386
28	1	0	3.128699	1.285973	0.543782
29	1	0	4.160601	1.440094	2.786628

30	1	0	3.120390	0.262146	4.716718
31	1	0	1.033335	-1.041964	4.363984
32	1	0	0.001837	-1.175345	2.161604
33	7	0	1.167400	1.141807	-1.009513
34	6	0	1.039766	0.004687	-0.275256
35	1	0	-1.367791	-0.287725	-0.412940
36	6	0	1.311844	-3.228308	-1.889877
37	7	0	1.580029	-2.472102	-2.902640
38	6	0	1.237167	-1.182774	-1.080875
39	7	0	1.096127	-2.505718	-0.750464
40	6	0	1.838131	-0.120862	-3.336700
41	6	0	0.642409	-3.106609	0.498443
42	1	0	1.255024	-4.306158	-1.919562
43	1	0	0.996861	0.566537	-3.393615
44	1	0	2.029496	-0.608356	-4.292111
45	1	0	2.710066	0.433046	-2.995078
46	1	0	-0.328430	-2.687536	0.787025
47	1	0	1.372582	-2.941346	1.289341
48	1	0	0.535205	-4.177053	0.316722
49	7	0	1.531383	-1.207128	-2.407698

Optimized Cartesian coordinates for 4-tsi1II

Center Number	Atomic Number	Atomic Type	Coordinates (Angstroms) X	Y	Z
1	6	0	1.571460	1.711412	0.660262
2	6	0	2.919499	1.502152	0.944443
3	6	0	3.860039	2.457547	0.576131
4	6	0	3.437269	3.609931	-0.080827
5	6	0	2.090267	3.813610	-0.390807
6	6	0	1.131400	2.857043	-0.003045
7	6	0	1.710243	5.056057	-1.128637
8	6	0	1.308634	5.047745	-2.482793
9	6	0	0.898420	6.252148	-3.069276
10	6	0	0.925675	7.449213	-2.365150
11	6	0	1.353071	7.455218	-1.041791
12	6	0	1.735454	6.263369	-0.432244

13	6	0	-0.322683	3.142763	-0.368111
14	7	0	-0.976759	4.218114	0.041764
15	6	0	1.279608	3.852277	-3.335897
16	6	0	2.007285	2.728157	-3.218066
17	6	0	1.815419	1.617545	-4.182686
18	6	0	2.466247	0.296002	-3.877863
19	6	0	3.029225	-0.006991	-2.633104
20	6	0	3.579558	-1.265583	-2.403008
21	6	0	3.580939	-2.223355	-3.413493
22	6	0	3.020024	-1.926543	-4.655563
23	6	0	2.460221	-0.676236	-4.883101
24	8	0	1.131892	1.740483	-5.185733
25	1	0	0.835341	0.985095	0.993354
26	1	0	3.226367	0.603337	1.471695
27	1	0	4.911987	2.313361	0.802523
28	1	0	4.159793	4.363395	-0.383382
29	1	0	0.567124	6.241179	-4.104499
30	1	0	0.609686	8.369470	-2.846259
31	1	0	1.367762	8.379416	-0.472224
32	1	0	2.019310	6.253467	0.616622
33	1	0	-0.497871	2.944840	-1.436279
34	1	0	0.602934	3.898110	-4.190422
35	1	0	2.746541	2.614583	-2.436420
36	1	0	3.022724	0.719873	-1.824688
37	1	0	4.010433	-1.492920	-1.432458
38	1	0	4.018030	-3.201270	-3.234898
39	1	0	3.019802	-2.672775	-5.444283
40	1	0	2.008651	-0.422849	-5.836995
41	6	0	-0.721089	4.751407	1.297456
42	6	0	-0.262457	4.032677	2.419772
43	6	0	-1.011318	6.119509	1.478544
44	6	0	-0.084312	4.663628	3.650243
45	1	0	-0.054983	2.970227	2.329862
46	6	0	-0.819035	6.743290	2.701056
47	1	0	-1.376297	6.667297	0.614274
48	6	0	-0.350329	6.020074	3.801174
49	1	0	0.268338	4.082731	4.498696
50	1	0	-1.040503	7.802441	2.803787

51	1	0	-0.203282	6.506831	4.760175
52	6	0	-2.556303	-0.099563	-0.846685
53	7	0	-3.345875	0.535315	-0.034793
54	6	0	-1.294233	1.502545	0.024365
55	7	0	-1.305637	0.453450	-0.846081
56	6	0	-3.136058	2.511342	1.368728
57	6	0	-0.164394	0.040875	-1.649850
58	1	0	-2.841575	-0.951553	-1.446272
59	1	0	-3.154786	3.471769	0.848881
60	1	0	-2.525173	2.610299	2.266893
61	1	0	-4.138380	2.166702	1.616808
62	1	0	-0.514034	-0.524351	-2.515355
63	1	0	0.527820	-0.568889	-1.064404
64	1	0	0.359315	0.934845	-1.994514
65	7	0	-2.549300	1.515183	0.483617

Optimized Cartesian coordinates for 4-tsIIIII

Center Number	Atomic Number	Atomic Type	Coordinates (Angstroms) X	Y	Z
1	6	0	-0.313670	0.905053	1.854532
2	6	0	-0.837706	0.211492	2.941412
3	6	0	-0.662766	-1.165590	3.032081
4	6	0	-0.000330	-1.830604	2.002328
5	6	0	0.486796	-1.152250	0.884426
6	6	0	0.365782	0.255439	0.812600
7	6	0	1.090435	-1.954625	-0.221331
8	6	0	0.439188	-2.105172	-1.467503
9	6	0	1.090650	-2.801649	-2.492696
10	6	0	2.327522	-3.400167	-2.283392
11	6	0	2.944484	-3.286789	-1.042283
12	6	0	2.332192	-2.559222	-0.025366
13	6	0	0.993845	1.043339	-0.284996
14	7	0	2.387299	0.825277	-0.813364
15	6	0	-0.897330	-1.560703	-1.755215
16	6	0	-1.927847	-1.481600	-0.898032
17	6	0	-3.212565	-0.878301	-1.323485

18	6	0	-4.277259	-0.678139	-0.285792
19	6	0	-3.992423	-0.660071	1.083327
20	6	0	-5.009051	-0.417376	2.003043
21	6	0	-6.313170	-0.207493	1.563852
22	6	0	-6.600983	-0.222143	0.198661
23	6	0	-5.585365	-0.445250	-0.721803
24	8	0	-3.404051	-0.508479	-2.472742
25	1	0	-0.395938	1.990210	1.833560
26	1	0	-1.353911	0.754055	3.728210
27	1	0	-1.035622	-1.717578	3.889198
28	1	0	0.122642	-2.910010	2.042604
29	1	0	0.599826	-2.893072	-3.458328
30	1	0	2.808404	-3.946700	-3.088598
31	1	0	3.918986	-3.732996	-0.869641
32	1	0	2.843361	-2.412423	0.923077
33	1	0	1.226379	0.362532	-1.273268
34	1	0	-1.080343	-1.231644	-2.779763
35	1	0	-1.838054	-1.856468	0.113463
36	1	0	-2.977059	-0.804876	1.442116
37	1	0	-4.778862	-0.394204	3.063919
38	1	0	-7.106024	-0.029353	2.284153
39	1	0	-7.617510	-0.055912	-0.144488
40	1	0	-5.780232	-0.445624	-1.789615
41	6	0	3.344911	0.347650	0.058799
42	6	0	3.310013	0.452902	1.465798
43	6	0	4.497364	-0.237153	-0.518343
44	6	0	4.361247	-0.032938	2.243748
45	1	0	2.454063	0.905729	1.955197
46	6	0	5.531849	-0.716572	0.263794
47	1	0	4.524889	-0.320391	-1.601136
48	6	0	5.472301	-0.630178	1.660245
49	1	0	4.300722	0.057637	3.325547
50	1	0	6.396622	-1.170465	-0.213830
51	1	0	6.280861	-1.013970	2.274020
52	6	0	-0.620048	4.160758	-1.053621
53	7	0	0.595178	4.599285	-0.944440
54	6	0	0.561445	2.392070	-0.504071
55	7	0	-0.705071	2.821556	-0.793128

56	6	0	2.743684	3.617587	-0.321384
57	6	0	-1.846152	1.949731	-1.007374
58	1	0	-1.472962	4.766311	-1.321951
59	1	0	3.305122	3.066510	-1.075961
60	1	0	2.963794	3.180897	0.657102
61	1	0	2.973652	4.681840	-0.329392
62	1	0	-1.568026	1.180568	-1.731744
63	1	0	-2.674168	2.542823	-1.397004
64	1	0	-2.144072	1.466047	-0.072248
65	7	0	1.321836	3.501138	-0.600837+-

Table S1: Calculated relative energies (all in kcal mol-1, relative to isolated species) for the ZPE-corrected Gibbs free energies (ΔG-gas), Gibbs free energies for all species in solution phase (ΔGsol) at 298 K by M06-2X/6-311++G(d,p)//M06-2X/6-31G(d) method and difference between absolute energy.

Species	ΔG_{gas}	$\Delta G_{sol(DMC)}$	$\Delta\Delta G_{sol-gas}$
i1	0.00	0.00	-28.98
ts-i1II	14.96	4.54	-39.39
II	8.50	-8.05	-45.52
ts-IIi2	27.24	1.39	-54.82
i2	9.54	-13.41	-61.73
ts-i2III	25.04	-7.71	-51.92
ts-IIi2-1	51.36	33.97	-46.37
i2-1	-10.75	-21.8	-32.34
ts-i2III-1	29.42	13.33	-41.22
III	-22.02	-27.66	-34.61
i3	0.00	0.00	-37.88
ts-i3IV	3.7	1.86	-42.43
IV	-18.54	-14.23	-40.17
i4	0.00	0.00	-74.78
ts-i45	14.43	2.98	-93.96
i5	-77.13	-76.28	-70.65
2V	-58.66	-68.25	-97.15
V-nhc	0.00	0.00	-48.58
2	-6.96	-10.16	-31.95
3-i1	0.00	0.00	-32.97
3-tsi1II	10.85	9.13	-40.39
3-II	3.17	3.56	-38.28
3-tsII III	43.55	40.38	-31.85
3-III	-13.97	-16.26	-40.96
4-i1	0.00	0.00	-29.86
4-tsi1II	17.09	4.76	-42.72
4-II	0.44	4.23	-48.05
4-tsII III	40.18	37.62	-41.51
4-III	-20.92	-20.77	-30.01

Table S2: The activation energy (local barrier) (in kcal mol-1) of all reactions in the gas, solution phase calculated with M06-2X/6-311++G(d,p)//M06-2X/6-31G(d) method and difference between the two.

TS	$\Delta G^{\neq}_{gas}$	$\Delta G^{\neq}_{sol}$	$\Delta\Delta G_{sol-gas}$
ts-i1II	15.0	4.5	-10.4
ts-IIi2	18.7	9.4	-9.3
ts-i2III	15.5	5.7	-9.8
ts-IIi2-1	42.9	42	-0.8
ts-i2III-1	40.2	35.1	-5
ts-i3IV	3.7	1.9	-1.8
ts-i45	14.4	3	-11.4
3-tsi1II	10.9	9.1	-1.7
3-tsIII II	40.4	36.8	-3.6
4-tsi1II	10.1	4.8	-5.3
4-tsIII II	39.7	33.4	-6.9

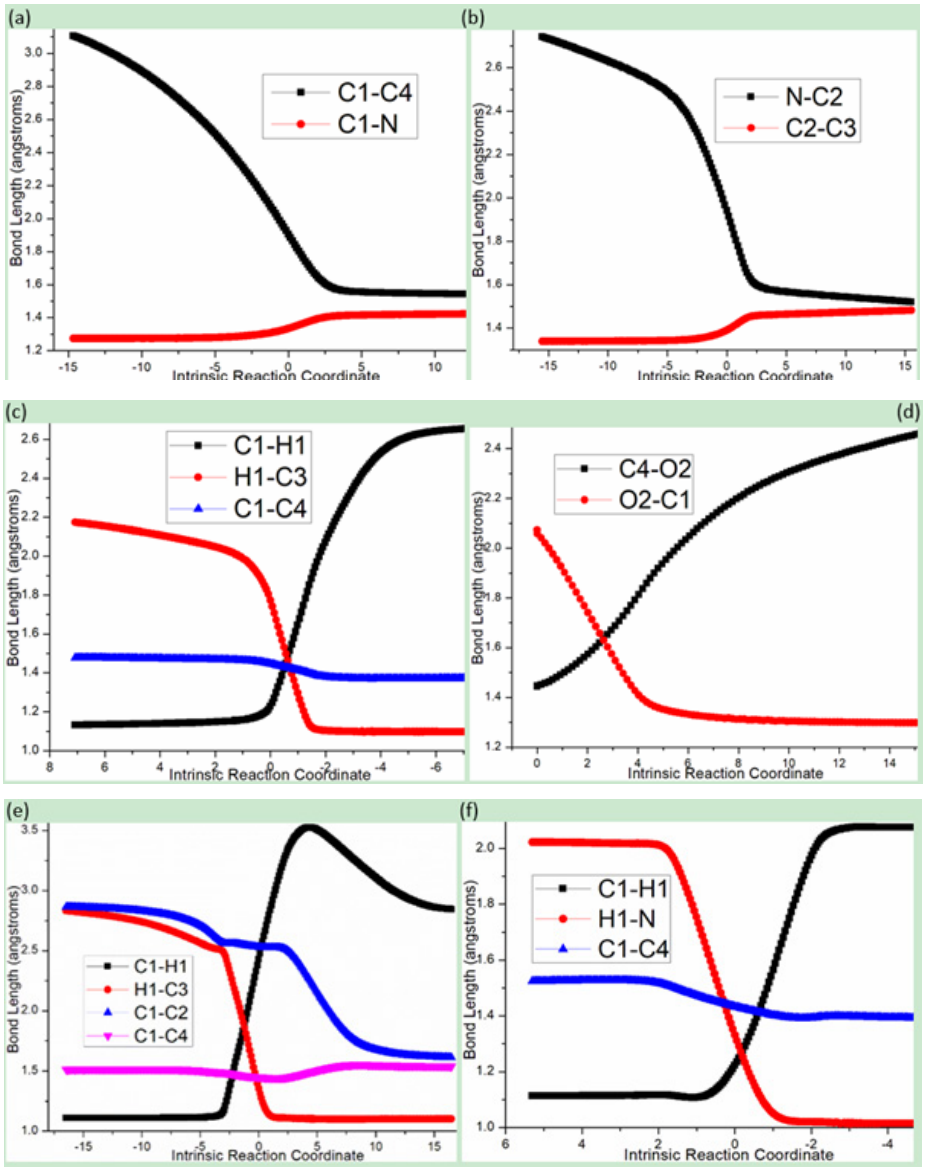

Figure S1: Evolution of bond lengths along the IRC for (a) **ts-i1II** (b) **ts-IIi2** (c) **ts-i2III** (d) **ts-i45** (e) **3-tsIIIII** (f) **4-tsIII II** at the M06-2X/6-311++G(d,p) level.